Conduction mechanism of hydrogenated nanocrystalline silicon films

Y. L. He
The National Laboratory of Solid State Microstructure Physics, Nanjing University, Nanjing 210093, China and The Amorphous Physics Research Lab, BUAA, Beijing 100083, China

G. Y. Hu
Department of Physics and Astronomy, Louisiana State University, Baton Rouge, Louisiana 70803

M. B. Yu
The Physics Department of Xi'an University of Technology, Xi'an 710048, China

M. Liu, J. L. Wang, and G. Y. Xu
The Amorphous Physics Research Lab, BUAA, Beijing 100083, China

(Received 3 September 1997; revised manuscript received 1 December 1998)

A heteroquantum dot (HQD) tunneling model for the conduction mechanism of hydrogenated nanocrystalline silicon films is proposed. The main features of the HQD model follow. (i) The micrograins and their amorphous counterparts have very different band gaps and band structures; as a result, they form a heterojunctionlike structure in interface regions where the band offset dramatically reduces the activation energy of electrons and the micrograins act as a quantum dot (QD). (ii) In the presence of an external field, activated electrons have ballistic properties in the QD's and quantum tunneling processes through the interface barriers. Based on this model, an equation for the conductivity of nc-Si:H films is deduced, and the calculated results are in good agreement with the experimental results. Using nc-Si:H thin layers a resonant tunneling diode with quantum characteristics was fabricated. [S0163-1829(99)11219-0]

I. INTRODUCTION

Low-dimensional silicon systems, such as porous silicon[1] and nc-Si/a-SiO_2 (nano silicon particles embedded in amorphous silica) are currently of considerable interest.[2,3] A common feature of these materials is the natural quantum confinement (NQC) due to the presence of nanoscale particles. The word ''natural'' used here distunguishes NQC from ''artificial'' quantum confinement (AQC), where an external gate bias is applied to produce the confinement.[4,5]

Also of interest, in the same context, are nc-Si:H films.[6–10] These nc-Si:H films are deposited by plasma-enhanced chemical-vapor deposition (PECVD) technology, which differs from a-Si:H film deposition only in the processing parameters. A typical nc-Si:H film is composed approximately of 50% nanocrystalline silicon with mean grain size 3–6 nm and 50% amorphous Si in the interface regions among the grains. The thickness of the interfaces is around 2–4 atomic spacings, but the constituent Si and H atoms are random and possess some unique elements.[11]

The two kinds of low-dimensional silicon systems mentioned above are disordered, i.e., the size and shape distribution of the nc grains are random. Therefore, we call them natural quantum confinement systems. In recent years, many novel characteristics have been found in the two kinds of low-dimensional silicon materisls: visible light emission from porous silicon and nc-Si/a-SiO_2, and a range of unusual properties and potential application for nc-Si:H films, e.g., high conductivity ($\sigma = 10^{-3}$–$10^{-1}\ \Omega^{-1}\,\mathrm{cm}^{-1}$) (even higher than that of C-Si), with excellent photo and thermal stability, ideal doping efficiency, and piezoresistive effects.[12]

Research on low-dimensional semiconductor systems has led to the development of quantum dot (QD) arrays on the scale of several hundreds or even several tens of nanometers on crystalline Si and GaAs wafers using photolithographic technology. Coulomb blockade effects, which are characteristic of single-electron effects, and quantum oscillation, etc., have also been observed in the liquid helium temperature range. Some of them have become the basis for the development of quantum function devices. However, their low operational temperature makes them of little practical value. The problem is to raise the quantum function temperature close to room temperature. A recent paper by Tsu,[2] in which microsilicon grains embedded in a-SiO_2 networks showed resonant tunneling characteristics close to room temperature, has therefore received much attention. The novelty is that for silicon grains of several nm in size in a disordered distribution, if their electrons are limited to the quantum dimension, some quantum effects such as Coulomb oscillation and resonant tunneling are observed at much higher temperatures than in AQCs.

We have also recently reported that microcrystalline silicon grains with a size of 3–6 nm in nc-Si:H films possess quantum dot characteristics both in their microstructures (see Fig. 1) and electrical properties. The high conductivity of the films comes mainly from conduction through the grains, while the interfaces are essentially insulating.[14] On this basis, we have developed tunneling diode devices from nc-Si:H thin layers (around 20 nm) and observed resonant tunneling, negative differential conductance (NDC), and quantum oscillation phenomena in the σ-V, I-V, and C-V characteristics at liquid nitrogen temperatures or below (<100 K).[15] This not

 ©1999 The American Physical Society

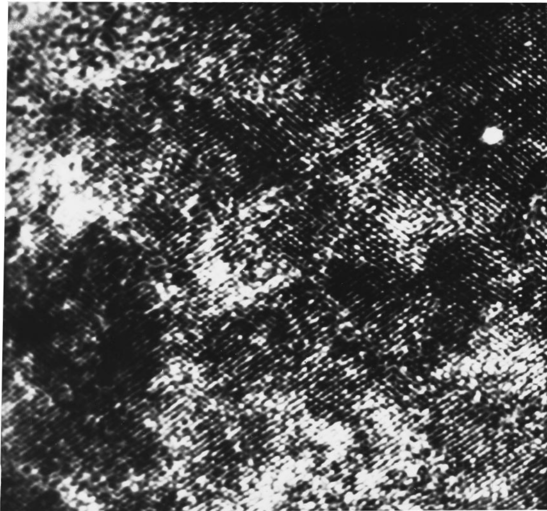

FIG. 1. The microstructure picture of nc-Si:H films (HREM).

only confirms Tsu's work but is also a discovery of quantum transport characteristics in nc-Si:H films.

In this paper, we discuss the quantum transport properties of nc-Si:H films. A conduction model is described in Sec. II, a single-electron tunneling model in Sec. III, the experimental evidence in Sec. IV, and some conclusions are presented in Sec. V.

II. A CONDUCTION MODEL FOR NC-SI:H FILMS—THE HETEROJUNCTION QUANTUM DOT TUNNELING, MODEL (HQD)

The model proposed for nc-Si:H films is based on the grain boundary trap (GBT) model for poly-silicon (pc-Si) films and developed from two main points:[16] First, by conceptually embedding silicon grains (QD) into Si networks to build nc-Si/a-Si systems and hence giving a qualitative description of their interface characteristics; and second, taking account of electron tunneling between grains, especially among nanocrystals. One result is that electron tunneling among silicon grains of nanoscale dimensions is related to single-electron transport.

It is known that artificial quantum dot (AQD) arrays are zero-dimensional electron systems, with confinement determined by an external gate bias.[5] The QDs in nc-Si:H films are natural quantum dots (NQDs),[7,9] whose size, shape, and distribution are arbitrary. The confinement characteristic of electrons in NQDs is similar in some aspects to that of AQDs, but there are also obvious differences. In AQDs, the QD arrays are regular and uniform matrixes, and the high potential barrier between QDs allows no opportunity for lateral transport within the arrays. In nc-Si/a-Si systems, however, the QD arrays are composed of QD networks of the isolated interface layers and of highly conducting nanoscale silicon grains separated in a disordered distribution. Hence, lateral transport will occur in nc-Si:H networks, because of the low potential barriers among grains with thin interface layers. Therefore, it is necessary to postulate a heterojunction quantum dot model to distinguish the basic quantum behavior in nc-Si/a-Si systems from that in AQD arrays. In the HQD model, the main physical concepts are as follows.

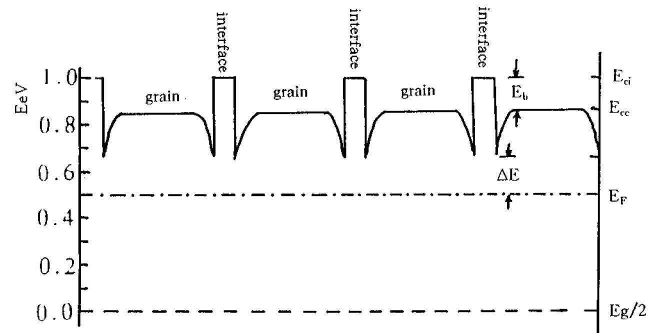

FIG. 2. The energy band diagram of nc-Si:H.

(1) The nanocrystalline grains and their interface regions made up of amorphous Si:H have very different band gaps and band structures (Fig. 2). As a result, they form heterojunction structures in which the band offset effect dramatically reduces the activation energy of electrons. This is an important reason why nc-Si:H films have high conductivities.

(2) In the presence of an external field, activated electrons have ballistic characteristics in silicon grains and quantum tunneling occurs through the interface barriers.

By means of Hall measurements the intrinsic nc-Si:H films have been proved to be n type,[9] with the Fermi level E_F close to the conduction band edge E_C. In addition, according to the GBT model, pc-Si is composed of small crystallites of size a bit more than 30 nm which are separated by a few disordered atomic layers of thickness around 1 nm, causing carrier trapping in the grains.[17] From electron spin resonance (ESR) measurements the density of neutral dangling bonds $N_t = 2.1\times 10^{17}$ cm^{-3}.[18] This is an order of magnitude lower than in μc-Si:H and pc-Si:H films. Since high concentrations of hydrogen ($C_H \cong 20$ at %) exist at grain boundaries in nc-Si:H films, it may compensate the dangling bonds.[19] Figure 2 shows the energy diagram of nc-Si:H, in which the energy edge offset is different from that in pc-Si. The energy edge offset of pc-Si is usually considered to be upward with a barrier height 0.5–1.0 eV. Evangelistic[20] calculated the hetrojunction band diagram of c-Si/a-Si and suggested that the offset at the valence band edge can be neglected due to the disorder at boundaries. Experimentally, however, there is a 0.1–0.2 eV offset at the conduction band edge.[16]

It is known that the energy gap E_g in both nanocrystalline silicon grains and the disordered interface region are different from that in bulk C-Si (1.15 eV) and in completely amorphous silicon films (1.7 eV). No reliable values of E_g in nc-SiH films have been reported to date. Therefore, we can only take the optical energy gap $E_g^{\rm opt}$ from our experimental resulsts to replace the interface energy gap ($E = 2.02$ eV) and the micrograin energy ($E = 1.7$ eV).[7,9] Hence, according to our HQD model the simple nc-Si:H diagram for the upper half of the energy band is shown in Fig. 2.

III. SINGLE-ELECTRON TUNNELING MECHANISM

According to our HQD model, the analysis for the single-electron conduction process in nc-Si:H films below will have a clear concept.

Using high-frequency transient capacitance spectra and

TABLE I. A series of experimental data for nc-Si:H films.

No.	X_c%	d (nm)	σ_{RT} (Ω^{-1} cm^{-1})	$\Delta E'$ (eV)	ΔE (eV)	ε_c (eV)
1	57	3.7	2.51×10^{-1}	0.14	0.10	0.16
2	55	3.5	6.56×10^{-2}	0.15	0.12	0.12
3	53	4.0	5.67×10^{-3}	0.17	0.12	0.20
4	51	6.0	3.27×10^{-3}	0.19	0.13	0.24
5	49	3.0	6.09×10^{-3}	0.18	0.14	0.16
6	47	4.5	6.37×10^{-3}	0.19	0.12	0.28

ESR measurements, respectively, we obtained the density of activated electrons, $n=10^{16}$–10^{17} cm^{-3}, and the density of deep energy levels in grains, $N_t=10^{17}$ cm^{-3}. These values are very small compared with the grain concentration (10^{18} cm^{-3}) in the film. On average, therefore, among tens or even hundreds of grains there is only one deep level and one electron. The electron may be trapped by deep levels in a boundary, causing the edge of the deep energy band in the boundary to bend downward. In this case, it is reasonable to consider the mechanism of conduction for QD arrays in nc-Si:H film to be a single-electron tunneling process, i.e., the electrons passing through the grains and tunneling through the interface barriers do so one by one. Therefore, in the HQD model the current carriers are thermally activated electrons in the interface regions between a-Si and nc-Si.

In the GBT model, the density of activated electrons is given by

$$n=n_0\exp(-\Delta E/KT), \tag{1}$$

where ΔE is the activation energy for nc-Si:H films and its experimental value is $\Delta E=(0.12$–$0.15)$ eV.[9] The constant n_0 is the electron density at the $T\rightarrow\infty$ limit. Using Eq. (1), the conductivity can be evaluated from $\sigma=ne\mu$, in which the electron mobility μ is normally temperature independent and the temperature dependence of the conductivity is solely determined by Eq. (1). The GBT model does not include the temperature dependence of electron tunneling in the network of heterojunction quantum dots. This must be taken into account.

Recently, Hu and O'Connell[21] adopted the Langevin model to study single-electron transport in a small tunneling junction. The result is helpful in our discussion of the HQD model. Electron tunneling is a complex process in HQDs. Assuming each dot has the same size, the same environment, and the same tunneling probability, the result derived by Cleland, Schmidt, and Clarke[22] can be used. The effective tunneling probability is

$$\langle\Gamma(Q)\rangle=\int_{-\infty}^{\infty}\Gamma(Q+q)P(q)dq \tag{2}$$

in which

$$P(q)=\frac{1}{\sqrt{2\pi\langle q^2\rangle}}\exp(q^2/2\langle q^2\rangle), \tag{3}$$

where $P(q)$ is the distribution function of electric charges calculated with the quantum Langevin equation, and the value of $\langle q^2\rangle$ is the mean square of the quantum distribution $P(q)$. The electron mobility μ, obtained by Hu *et al.*[16] is

$$\mu=\mu_0\int_{-\infty}^{+\infty}dq\,P\left[\frac{1}{1-e^{\beta\Delta E^+}}\left(1+\frac{\beta\Delta E^+}{e^{-\beta\Delta E^+}-1}\right)+\frac{1}{1-\varepsilon^{\beta\Delta E^-}}\left(1+\frac{\beta\Delta E^-}{e^{-\beta\Delta E^-}-1}\right)\right]=\mu_0F(\langle q^2\rangle,T), \tag{4}$$

where $\beta=1/KT$. The energy $\Delta E^{\pm}$ given in Eq. (5) is the change in the charging energy caused by electron tunneling,

$$\Delta E^{\pm}=\left(1\pm\frac{2q}{e}\right)\frac{e^2}{2C}\equiv\left(1\pm\frac{2q}{e}\right)\varepsilon_c. \tag{5}$$

Notice that the integration in Eq. (4) represents the charging function for quantum dots as a result of single-electron tunneling. It tends to 1 at $T\rightarrow\infty$. Thus from Eqs. (1) and (4) the conductivity formula for nc-Si:H is written as the following:

$$\sigma=ne\mu=\sigma_0\exp[-\Delta E/k\ T]F(\langle q^2\rangle,T) \tag{6}$$

in which

$$\sigma_0=n_0e\mu_0$$

and

$$F(\langle q^2\rangle,T)$$

is the integrated in Eq. (4). Equation (6) is the complete conductivity expression in nc-Si:H films in the HQD model. It is the main result of this paper and it shows clearly that the

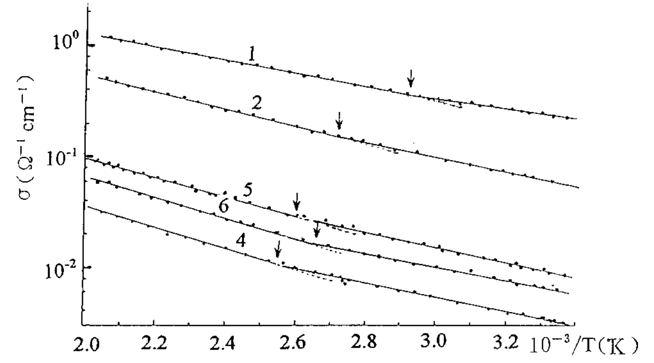

FIG. 3. The Arrhenius curves of nc-Si:H films.

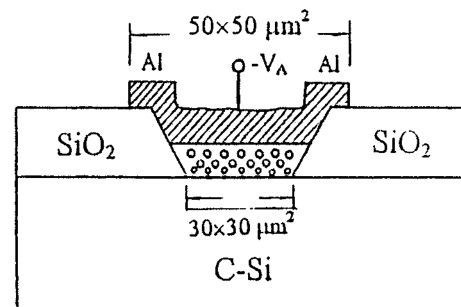

FIG. 4. Schematic diagram of nc-Si:H tunneling diode (TD).

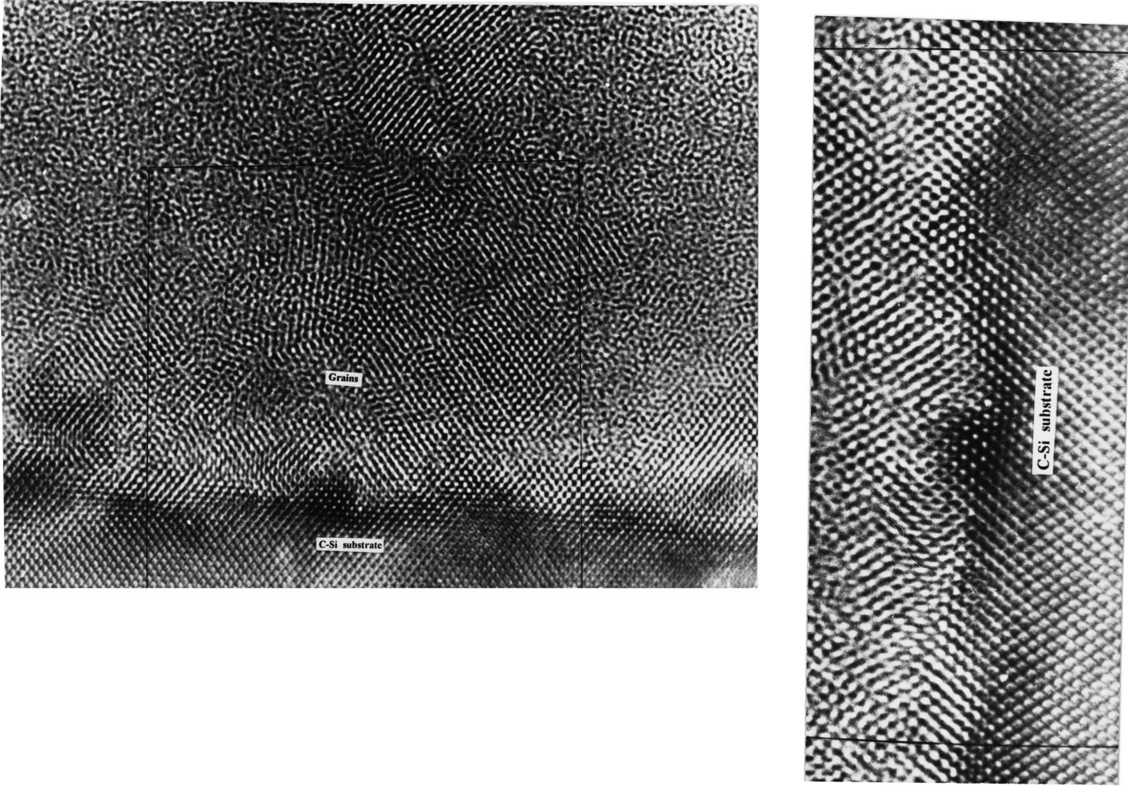

FIG. 5. HREM photograph of thin nc-Si:H films on C-Si substrate.

conductivity of nc-Si:H films has a complicated temperature behavior, i.e., it depends on the activated process as a well tunneling process. In the low-temperature region ($\varepsilon_c \gg KT$), the factor F of Eq. (4) can be evaluated explicitly and Eq. (6) can be simplified to

$$\sigma = \sigma_0 \exp[-\Delta E/k\,T]\mathrm{erfc}\left(\frac{e}{\sqrt{8\langle q^2\rangle}}\right)$$
$$\rightarrow \sigma_0 \sqrt{\frac{8\langle q^2\rangle}{\pi e^2}}\exp\left[-\frac{\Delta E}{k\,T}-\frac{e^2}{8\langle q^2\rangle}\right]. \quad (7)$$

where the quality $\langle q^2\rangle$ is related to features of the tunneling junction and can be calculated from the quantum Langevin equation. From Ref. 16, we have

$$\frac{\langle q^2\rangle}{e^2} = \frac{KT}{2\varepsilon_c}\coth\left(\frac{KT}{2\gamma\varepsilon_c}\right), \quad (8)$$

where γ is the value of $\langle q^2\rangle/e^2$ at the $T\rightarrow 0$ limit. We note that a critical temperature is defined in Eq. (8), $2\gamma\varepsilon_c = KT$, which separates the classical and quantum behavior for $\langle q^2\rangle$. In the case of $\langle q^2\rangle/e^2 = KT/2\varepsilon_c$, we get the following.

(1) In the quantum limit case, $2\gamma\varepsilon_c > KT$, then $\langle q^2\rangle/e^2$ tends to a constant and is insensitive to temperature. Here, Eq. (7) can be reduced to

$$\sigma = \sigma_0 \exp(-\Delta E/KT). \quad (9)$$

(2) In the classical limit case, $2\gamma\varepsilon_c < KT < \varepsilon_c$ and $\langle q^2\rangle/e^2 = KT/2\varepsilon_c$, and we can obtain

$$\sigma \sim \exp\left[-\frac{\Delta E + \varepsilon_c/4}{KT}\right] = \exp\left(-\frac{\Delta E}{KT}\right)\left[A + B\exp\left(-\frac{\varepsilon_c}{KT}\right)\right]. \quad (10)$$

(3) In the intermediate-temperature range, the conductivity σ is a complicated function of γ, ΔE, and ε_c. It is discussed in Ref. 16.

The results discussed indicate that there are two different values of the activation energy for conduction ΔE and $\Delta E' = \Delta E + \varepsilon_c/4$. This is an important result from the HQD model, and is quite different from that of the GBT model.

IV. EXPERIMENTAL EVIDENCE FOR THE HQD MODEL

According to the discussion mentioned above, we can calculate the Coulomb charging energy $E_c = e^2/2\mathrm{C} = (0.1\text{–}0.2)$ eV and the activation energy for conduction $\Delta E = (0.1\text{–}0.2)$ eV for nc-Si:H films on the condition that the mean grain size is 3–6 nm and the capacitance for each grain is $C = (5\text{–}8)\times 10^{-19}$ F. Moreover, we have measured for conductivity for many samples and analyzed the results. Some typical results are listed in Table I, and shown graphically in the Arrhenius plots in Fig. 3. In Fig. 3 each line has a weak kink point around 150–180 °C. From the slope of the Arrhenius plot above the kink point, we can derive conduction activation energy $\Delta E' = \Delta E + \varepsilon_c/4$, and from below the kink point the activation energy ΔE. Hence, from the experimental data we deduce that $\varepsilon_c = (0.16\text{–}0.28)$ eV, which is very close to the theoretical prediction: (0.1–0.2) eV.

In Table I, it is shown that the conductivity of nc-Si:H films at room temperature has a range $\sigma = (10^{-3}\text{–}10^{-1})\ \Omega^{-1}\,\mathrm{cm}^{-1}$. The conductivity is increased

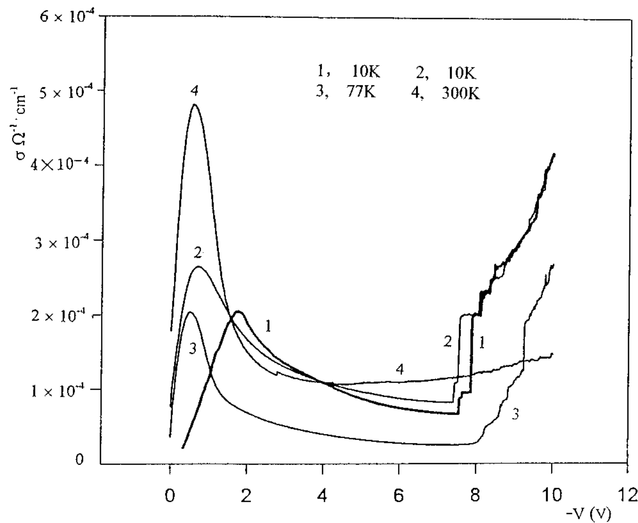

FIG. 6. σ-V characteristic curves of TD.

logarithmically with X_c (Ref. 9) in the range of volume crystallites $X_c=(53\pm5)\%$ and with mean grain size $d=(3-6)$ nm. Note that the X_c value of the No. 4 sample is larger than that of No. 5 and No. 6, but its σ value is lower. Through careful observation, it was found that the mean grain size of No. 4 is bigger than that of No. 5 and No. 6, so its σ value is lower. This is an important feature of nc-Si:H films: the so-called ''small size effect'' in the conduction process.[14]

To further observe and confirm QD characteristics and the HQD transport mechanism of the micrograins in nc-Si:H films, we selected a thin layer of nc-Si:H film (20 nm) to make a tunneling diode structure. First, a SiO_2 layer around 200 nm in thickness was prepared by thermal oxidation of an n-type C-Si(100) wafer at 1020 °C (the resistivity of the wafer was about 1 Ω cm). The SiO_2 layer was etched and patterned by photolighography to make an array of square holes (30 μm×30 μm). After appropriate treatment, a fresh nc-Si:H layer around 20 nm in thickness was deposited on the array configuration. The outer layer of the nc-Si:H films in the square holes was removed by etching and photolithography, leaving only very thin nc-Si:H layers in the hole bottoms. In the last step Al electrodes were (50 μm×50 μm) evapaorated on each square. The whole structure is shown in Fig. 4. The microstructure of the film was examined by high-resolution transmission microscopy (HREM) to confirm that the thin nc-Si:H layers (20 nm), directly deposited on the C-Si substrate, were really nanocrystalline in structure. A HREM picture is shown in Fig. 5, without the amorphous buffer layer between the C-Si substrate and thin nc-Si:H film. It verifies the nanostructure of the thin film.

A dc electrical bias was applied to the devices, with the Al electrode negative and σ-V, I-V, and C-V characteristics were measured at 1 MHz frequency in the temperature range from 10 K to room temperature. Typical σ-V, I-V, and C-V curves are shown in Figs. 6, 7, and 8. With the increasing negative bias voltage in the range of 0–2 V, there is a peak in the σ-V curves and the peak is shifted to lower bias as the temperature is raised from 10 to 300 K. The height for the peak is increased correspondingly. In the bias range of −2 to −7 V, there is a wide negative resistance valley. In the −7 to −9 V range there is a series of equally spaced quantum staircases in the temperature region 10–77 K. Figure 7 shows the I-V curves in the bias range of −7 to −9 V. Figure 8 shows some oscillatory discontinuities in the same bias range on the C-V curves. When the temperature is higher than 100 K, the staircases on σ-V and I-V curves, and the oscillatory discontinuities of the C-V curve, disappear and return to normal. These results are similar to those of Fig. 4 in Ref. 13. Therefore, these experiments directly prove the special characteristics of the HQD for micrograins in nc-Si:H film. The quantum oscillation phenomena appear in the liquid nitrogen temperature range, and hence there are promising applications for this nc-Si:H material.

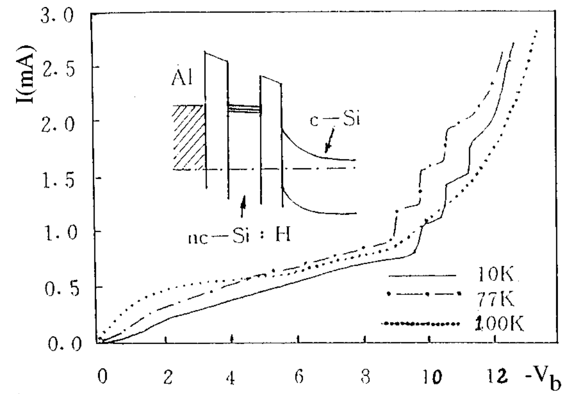

FIG. 7. I-V characteristic curves of TD.

V. CONCLUSION

The nanocrystalline silicon films (nc-Si:H) were deposited with a conventional PECVD method under conditons of well-controlled process parameters. From microstructure or electrical properties, the micrograins in 3–6 nm of thin films show the characteristics of quantum dots. The differences between NQD and AQD have been analyzed in detail in this paper. So, the HQD tunneling model has been introduced for qualitative and quantitative description.

The HQD tunneling model was developed from the grain boundary trapping model and complemented by adding quantum behaviors for nano micrograins in nc-Si:H films. A single-electron tunneling process is discussed and a complete conductivity formula for nc-Si:H films is presented. The

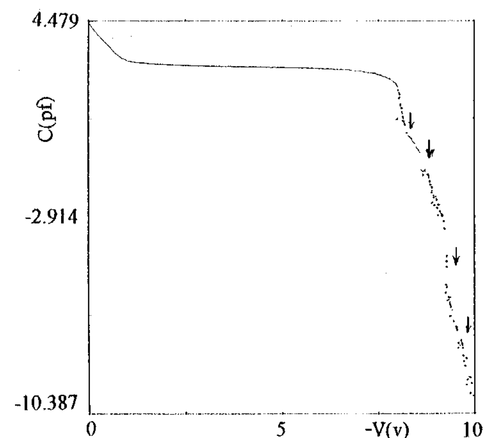

FIG. 8. C-V characteristic curve of TD.

transport mechanism of the HQD model is, single electrons have ballistic motion inside grains and tunnel through the interface barriers to form an overall conduction route. The main results of the HQD model are that in the low-temperature limit ($\varepsilon_c \gg K$T, in quantum transport range) and the high-temperature limit ($\varepsilon_c \ll$KT, as classical limit), there are two distinct conduction transport processes and two different activation conduction energies. The values ΔE and E_c calculated theoretically from the HQD model are in agreement with experimental measurement data. Data listed in this paper show that the quantum operational temperature for NQD films is much higher than that of AQD films. So, nc-Si:H films will be more practical for further application.

ACKNOWLEDGMENTS

This research work was supported by the National Foundation of Nature Science of China.

[1] L. T. Canham, Appl. Phys. Lett. **57**, 1046 (1990).

[2] R. Tsu, Physica B **189**, 325 (1993).

[3] Jane G. Zhu, C. W. White, J. D. Budai, S. P. Withrow, and Y. Chen, J. Appl. Phys. **78**, 4386 (1995).

[4] U. Merkt, Adv. Solid State Phys. **30**, 77 (1990).

[5] Y. Wang and S. Chou, Appl. Phys. Lett. **63**, 2257 (1993).

[6] M. Konuma, H. Curtins, F. A. Sarott, and S. Veprek, Philos. Mag. B **55**, 377 (1987).

[7] He Yuliang, Liu Xiangna, Wang Zhichao, Cheng Guangxi, Wang Luchun, and Yu Shidong, Sci. China, Ser. A **36**, 248 (1993).

[8] He Yuliang, Chu Yiming, Lin Hongyi, and Jiang Shusheng, Chin. Phys. Lett. **10**, 539 (1993).

[9] Yuliang He, Chengzhong Yin, Guangzu Cheng, Luchun Wang, Xiangna Liu, and G. Y. Hu, J. Appl. Phys. **75**, 797 (1994).

[10] P. Broguerira, J. P. Cone, S. Arekat, and V. Chu, J. Appl. Phys. **79**, 8748 (1996).

[11] C. L. Bai, Z. H. Wang, C. C. Dai, P. C. Zhang, and Y. L. He, J. Vac. Sci. Technol. B **12**, 1823 (1994).

[12] Yuliang He, Hong Liu, Mingbin Yu, and Xizomei Yu, Nanostruct. Mater. **7**, 769 (1996).

[13] Q. Ye, R. Tsu, and E. H. Nicollian, Phys. Rev. B **44**, 1806 (1991).

[14] Yuliang He, Yayi Wei, Guoxhen Zheng, Mingbin Yu, and Ming Liu, J. Appl. Phys. **82**, 3408 (1997).

[15] He Yuliang, Yu Mingbin, Lu Yanwu, Rong Ailian, Liu Jian, Xu Shijia, Luo Kejian, and Xe Zhonghe, Prog. Nat. Sci. **6**, 700 (1996).

[16] G. Y. Hu, R. F. O'Conell, Y. L. He, and M. B. Yu, J. Appl. Phys. **78**, 3845 (1995).

[17] J. Y. W. Seto, J. Appl. Phys. **46**, 5247 (1975).

[18] H. N. Liu, Y. L. He, F. Wang, and S. Grebner, J. Non-Cryst. Solids **164&166**, 1005 (1993).

[19] G. Harbeke, *Polycrystalline Semiconductors* (Springer-Verlag, Berlin, 1985).

[20] F. Evangelistic, J. Non-Cryst. Solids **78&79**, 969 (1985).

[21] G. Y. Hu and R. F. O'Connell, Phys. Rev. B **46**, 14 219 (1992).

[22] A. N. Cleland, J. M. Schmidt, and J. Clarke, Phys. Rev. B **45**, 2950 (1992).